Inorganic Chemistry

Article

pubs.acs.org/IC

Titanium–Oxo Cluster with 9-Anthracenecarboxylate Antennae: A Fluorescent and Photocurrent Transfer Material

Yin-Yin Wu,[†] Xiao-Wen Lu,[†] Miao Qi,[†] Hu-Chao Su,[†] Xiao-Wei Zhao,[†] Qin-Yu Zhu,*[,†,‡] and Jie Dai*[,†,‡]

[†]College of Chemistry, Chemical Engineering and Materials Science, Soochow University, Suzhou 215123, People's Republic of China

[‡]State Key Laboratory of Coordination Chemistry, Nanjing University, Nanjing 210093, People's Republic of China

Supporting Information

ABSTRACT: Attention has been paid to titanium–oxo clusters (TOCs) modified with functional molecules, because they can be considered as model systems for dye-sensitized titanium oxides in terms of their information in structures and electron transfer. We select 9-anthracenecarboxylate (9-AC) as a photoactive ligand and prepare two model compounds, $[Ti_6O_6(O^iPr)_6(9\text{-}AC)_6]$ (**1**) and $[Ti_6O_4(O^iPr)_6(cat)_4(9\text{-}AC)_2]$ (**2**) (where cat = catecholate). Structures of the TOCs and the dye–TOC linkage are characterized by single-crystal analysis. Solvent-induced fluorescence change is observed for the cluster solution, and the fluorescence can be turned off by irradiating and on by oxygen bubbling. Photoinduced Ti(III) is responsible for the fluorescence extinction. The photocurrent conversion property of the clusters is examined by use of a three-electrode cell with cluster-coated indium tin oxide (ITO) electrodes. The results indicate that 9-AC is an effective photosensitizer and cluster **1** shows higher photocurrent intensity for its multiantenna structure in comparison with that of **2**. Density of states for cluster **1** is calculated, in which the discrete energy bands of Ti_6O_{24} include a number of new energy levels for the contribution of 9-AC molecules.

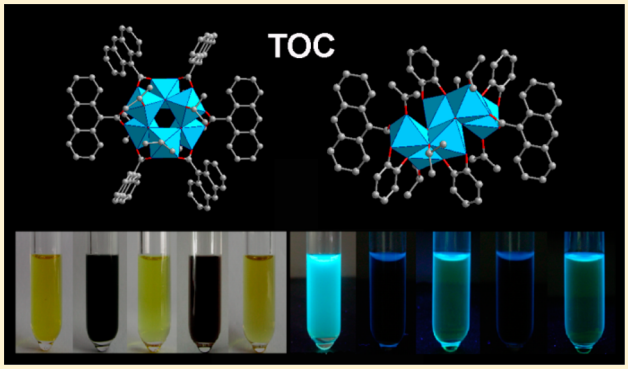

INTRODUCTION

Dye-sensitized solar cells (DSSC) have attracted great interest in the conversion of sunlight to electricity due to their low cost and high efficiency.[1] The properties of photosensitive dyes adsorbed on TiO surfaces have been extensively investigated. From a phenomenological standpoint, much is now understood about what goes on in a DSSC.[2] The working principle of photoelectricity conversion for DSSCs is essentially the light-induced excitation of the dye molecule from its ground state to the excited state and then interfacial electron transfer from the excited molecular sensitizer to the semiconductive nanoparticle.[3] However, accurate microscopic images of structures and energetics, at an atomic level of detail, have been much more difficult to reveal, which has stimulated a tremendous effort by the theoretical research community to better understand its microscopic details.[4] Theoretical studies on such aspects are mainly performed on the basis of theoretical TiO models of periodic boundary or cluster, which are not amenable to standard techniques like X-ray diffraction analysis. Hence, insight into dye–semiconductor binding and electronic structure with accurate structural information is important for reliable research results.

Titanium–oxo clusters (TOCs) can be considered as model compounds for bulk nanoscale titanium oxides in terms of their clear information on crystal structures.[5,6] Recently, dye molecule-functionalized TOCs have been paid extra attention due to the applications of dye-sensitized titanium oxide materials and have been used as models for studies of dye–TiO_2 bonding structures, excitation of the bonded dyes, and charge or electron transfer.[7] The crystalline TOCs offer the opportunity to bridge the practical dye-sensitized TiO_2 nanomaterials and the theoretical models in terms of both atomic structures and electronic states. TOCs with catechol were reported by Benedict and Coppens,[7a] and the clusters exhibited a red color due to penetration of the highest occupied catechol levels into the band gap of the TOCs. Theoretical simulations of electron transfer in polyoxotitanate nanoclusters Ti_{17} $[Ti_{17}O_{24}(O^iPr)_{20}]$ functionalized with nitrophenyl acetylacetone, of which the structures were fully established by X-ray diffraction measurements, are presented by Snoeberger ey al.[7b] We reported a Co^{II}phen moiety fused Ti_{17}–oxo cluster, and the single-crystal structure was successfully solved. As a model, the density states, photocurrent response, and complex–cluster electron transition were discussed.[7c] Nevertheless, reports based on such model clusters with dye molecules are still scarce.

Received: February 17, 2014
Published: June 20, 2014

   dx.doi.org/10.1021/ic500390j | Inorg. Chem. 2014, 53, 7233–7240

Anthracene group is a well-known fluorescent moiety, which is used widely in photoactive systems.[8] Theoretical studies on the TiO-9-AC (9-anthracenecarboxylate) system[9] and solar energy cells with the 9-AC-adsorbed TiO_2 electrode have been carried out.[10] We recently selected 9-AC as a functional organic dye ligand to prepare TOC model compounds for studies of the structures, optical and electrical properties, and electron transfer between 9-AC and TiO_2 particles. This is a convenient system for study because the dye molecule has a carboxylate group that can strongly bond to the TiO skeleton by replacing the simple acetate group in $[Ti_xO_y(OR)_z(OAc)_w]$-type clusters.[5] We successfully integrate the TOC with 9-AC in a unique structure and two clusters, $[Ti_6O_6(O^iPr)_6(9\text{-}AC)_6]$ (**1**) and $[Ti_6O_4(O^iPr)_6(cat)_4(9\text{-}AC)_2]$ (**2**) (where cat = catecholate), are first prepared and characterized by single-crystal analysis. Accurate crystal structures and bonding information on the dye on TiO_2 semiconductor are revealed. The work described here is also aimed at exploring their fluorescence properties and application of the clusters as a precursor in preparation of a photoelectroactive electrode. Preliminary study on the electronic states and electron transition of this system are discussed.

EXPERIMENTAL SECTION

General Remarks. All analytically pure reagents were purchased commercially and used without further purification. Elemental analyses of C, H, and N were performed on a Varidel III elemental analyzer. The Ti content was obtained by X-ray photoelectron spectroscopy (XPS). XPS measurements were recorded on an Escalab 250Xi spectrometer. Fourier transform infrared (FT-IR) spectra were recorded as KBr pellets on a Nicolet Magna 550 FT-IR spectrometer. ^{1}H NMR spectra were measured in $CDCl_3$ with tetramethylsilane, $Si(CH_3)_4$, as an internal standard on a UnityNova-400 spectrophotometer. Solid-state room-temperature optical diffuse reflectance spectra of the micro crystal samples were obtained with a Shimadzu UV-3150 spectrometer. Fluorescence was recorded on an Edinburgh FLS920 fluorescent photometer. Room-temperature X-ray diffraction (XRD) data were collected on a D/MAX-3C diffractometer using a Cu tube source (Cu Kα, λ = 1.5406 Å). The morphologies of the electrode films were observed with a JSM-5600LV scanning electron microscope (SEM). Solid-state ESR spectra were recorded by an EMX-10/12 spectrometer at 110 K with the frequence 9.4896 GHz. Thermogravimetric analyses were carried out with a SDT 2960 thermal analyzer. The samples were heated under a nitrogen stream of 100 mL/min with a heating rate of 20 °C/min.

Syntheses. *$[Ti_6O_6(O^iPr)_6(9\text{-}AC)_6]$ (1).* Analytically pure $Ti(O^iPr)_4$ (0.1 mL, 0.26 mmol) and 9-anthracenecarboxylic acid (45 mg, 0.020 mmol) were mixed in 0.5 mL of anhydrous CH_3CN. The mixture was placed in a thick Pyrex tube (0.7 cm dia., 18 cm length) and quickly degassed by argon. The sealed tube was heated under autogenous pressure at 100 °C for 3 days, and then cooled to room temperature to yield yellow-brick crystals [50% yield based on $Ti(O^iPr)_4$]. The crystals are rinsed with ethanol and dried. The compound was preserved under a sealed and dry environment. Anal. Calcd for $C_{108}H_{96}O_{24}Ti_6$ (MW 2065.25): C, 62.81; H, 4.69; Ti, 13.91. Found: C, 62.55; H, 4.92; Ti, 13.72. ^{1}H NMR ($CDCl_3$, δ ppm) 8.43 (d, AC), 8.05 (s, AC), 7.55 (d, AC), 6.93 (t, AC), 6.44 (t, AC); 3.65 (m, ^{i}Pr), 1.46 (d, ^{i}Pr). Important IR data (KBr, cm^{-1}): 3048(w), 2970(m), 2930(w), 2870(w), 1620(w), 1586(s), 1540(m), 1440(s), 1387(vs), 1330(s), 1130(s), 1010(m), 872(m), 721(vs), 663(s), 602(m), 474(s).

$[Ti_6O_4(O^iPr)_6(cat)_4(9\text{-}AC)_2]$ (2). Analytically pure $Ti(O^iPr)_4$ (0.1 mL, 0.26 mmol), 9-anthracenecarboxylic acid (35 mg, 0.016 mmol), and catechol (50 mg, 0.045 mmol) were mixed in 0.5 mL of anhydrous toluene. The mixture was placed in a thick Pyrex tube and quickly degassed by argon. The sealed tube was heated under autogenous pressure at 100 °C for 5 days, and then cooled to room temperature to yield red crystals [60% yield based on $Ti(O^iPr)_4$]. The crystals were rinsed with ethanol and dried. The compound was preserved under a sealed and dry environment. Anal. Calcd for $C_{72}H_{76}O_{22}Ti_6$ (MW 1580.66): C, 54.71; H, 4.85; Ti, 18.17. Found: C, 54.42; H, 4.75; Ti, 18.43. ^{1}H NMR ($CDCl_3$, δ ppm): 8.49 (s, AC), 8.43 (d, AC), 7.96 (d, AC), 6.79 (t, AC), 6.62 (t, AC), 6.44 (d, Cat), 6.10 (d, Cat), 4.55 (m, ^{i}Pr), 4.03 (m, ^{i}Pr), 1.58 (d, ^{i}Pr), 1.52 (d, ^{i}Pr). Important IR data (KBr, cm^{-1}): 3053(w), 2977(m), 2926(w), 2870(w), 1618(w), 1581(w), 1530(s), 1480(vs), 1424(s), 1382(s), 1322(s), 1258(vs), 1106(vs), 1006(s), 884(m), 819(s), 703(vs), 625(s), 575(s), 481(s).

X-ray Crystallographic Study. The measurements were carried out on a Rigaku Mercury charge-coupled device (CCD) diffractometer with graphite monochromated Mo Kα (λ = 0.710 75 Å) radiation. X-ray crystallographic data for all compounds were collected and processed by use of CrystalClear (Rigaku).[11] The structures were solved by direct methods with the SHELXS-97 program and the refinement was performed against F^2 with SHELXL-97.[12] All non-hydrogen atoms are refined anisotropically. The hydrogen atoms are positioned with idealized geometry and refined with fixed isotropic displacement parameters. Detailed crystal data and structural refinement parameters for **1** and **2** are listed in Table S1 in Supporting Information.

Fluorescence Quenching Measurement. A 70-W halogen lamp was employed as light source, which was positioned 15 cm over the surface of the solution in a quartz cuvette. The cuvette should be covered to keep the solution in the absence of O_2. The concentration of the solution was about 1.0×10^{-4} mol·dm^{-3}. The fluorescence intensity was tracked with 10-min intervals of irradiation, until the fluorescence was quenched. Then O_2 was bubbled into the solution to recover the fluorescence.

Film Preparation and Photocurrent Measurement. Films of clusters **1** and **2** were prepared by solution coating method. The new prepared clusters (0.01 mmol) were dissolved in 2 mL of CH_2Cl_2 solvent. The solutions were transferred to a glass syringe and then dropped on the cleaned glass plate for SEM measurement, or on indium tin oxide (ITO) glass (100 Ω/□) for photocurrent measurements. The coating films were obtained after the solvent was carefully removed by evaporation and dried under reduced pressure. A 150-W high-pressure xenon lamp, positioned 15 cm from the surface of the ITO electrode, was employed as a light source. The photocurrent experiments were parallel performed on a CHI650 electrochemistry workstation in a three-electrode system, with the sample-coated (in Φ = 0.8 cm area) ITO glass as the working electrode, a Pt wire as the auxiliary electrode, and a saturated calomel electrode (SCE) as the reference electrode. An aqueous solution of Na_2SO_4 (100 mL, 0.10 mol·dm^{-3}) was used as the medium in a quartz cell.

RESULTS AND DISCUSSION

General and Structural Characterization. Crystals of clusters **1** and **2** were prepared directly by one-step in situ solvothermal synthesis at 100 °C for 3−5 days in anhydrous CH_3CN or toluene (see Experimental Section). Cluster **1** was obtained as greenish-yellow crystals and cluster **2** was obtained as red crystals (Figure 1a and 1b). Solid-state UV−vis absorption spectra of the clusters, calculated from diffuse-reflectance spectra, show a broad absorption band around 3.3 eV, which is the representative band of anthracene (Figure 1c). The onset energy of **1** is 2.72 eV (456 nm, yellow), part covering the visible range, while that of **2** is 2.05 eV (605 nm, red) due to the charge transfer (CT) from catecholate to cluster core.[7a] The dye coordination, especially the CT band, improves the absorption property of the clusters for visible light, because the onset energy of pure TOCs is about 3.5 eV.[7c] This phenomenon has been tested for the CT-induced dye-sensitized solar cell,[13a] and the related CT interaction has also been employed to assay the surface acidity of various metal oxides.[13b] FT-IR spectra of clusters **1** and **2** are shown in Figure

dx.doi.org/10.1021/ic500390j | Inorg. Chem. 2014, 53, 7233−7240

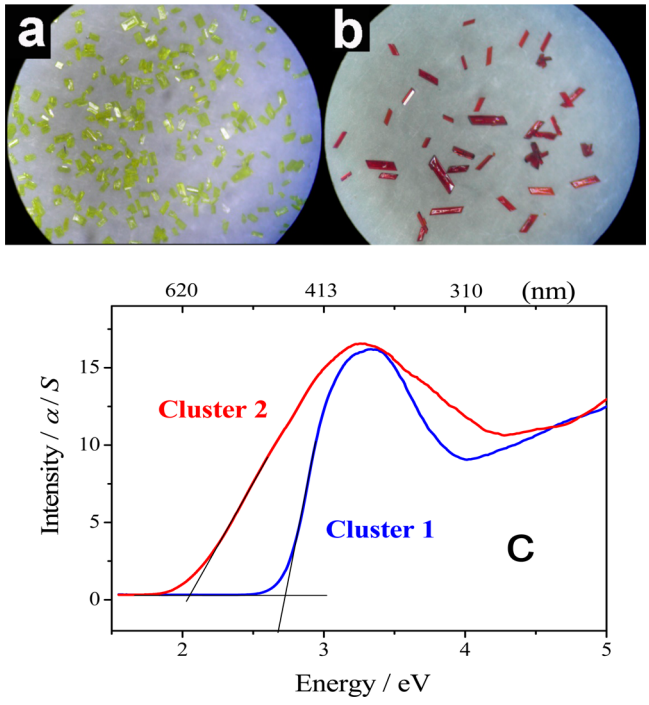

Figure 1. Crystals of clusters (a) **1** and (b) **2**. (c) Solid-state UV−vis absorption spectra of **1** (blue curve) and **2** (red curve).

S1 (Supporting Information). The vibrations, 1586 and 1387 cm^{-1} for **1** and 1530 and 1382 cm^{-1} for **2**, indicate the chelating coordination of the carboxyl group. Isopropoxy groups are detected by the ν_{C-H} (between 2970 and 2850 cm^{-1}) and ν_{Ti-O-C} (1010 and 1006 cm^{-1}) vibrations. The bands around 720 cm^{-1} are attributed to Ti−O vibrations. The bands about 3050, 1550, 1450, and 710 cm^{-1} are assigned to the characteristic bands of the C−H stretches of the aromatic planes. The XRD patterns of the bulk microcrystal samples are in agreement with those simulated from the data of single-crystal analysis (Figure S2, Supporting Information). Thermogravimetry analysis (Figure S3, Supporting Information) indicates no cocrystallized solvent, because the temperature of the first inflection of the curve is 250 °C. Clusters **1** and **2** decomposes in two steps, corresponding with the removal of 2-propanol and decomposition of 9-AC. Finally, TiO_2 formed at the temperature about 500 °C.

The structures of **1** and **2** were characterized by single crystal X-ray analysis. Ball−stick plots of the structures are shown in Figure 2, along with polyhedron views of the Ti_6O_{24} and Ti_6O_{22} cluster structures, respectively. The structures of **1** and **2** with thermal ellipsoid plots are provided in Supporting Information (Figure S4). A number of titanium−oxo clusters with the same D_{3d} Ti_6O_6 core as in **1** were reported, $[Ti_6O_6(OR)_6(O_2CR')_6]$.[14] The core structure shows two stacked six-membered rings consisting of alternating titanium and oxygen atoms. The unique characteristic of **1** is the six large antenna groups of anthracene that surround the Ti_6O_6 core like a paddle wheel. Cluster **2** consists of a central symmetric assembly of two Ti_3O_{13} units built by three edge-shared octahedra. Two 9-AC ligands coordinate to the core in opposite, and the other four carboxyl sites are replaced by the catecholate. The clusters are assembled to a one-dimensional structure by $\pi\cdots\pi$ stacking (3.371 Å, Figure 3a)

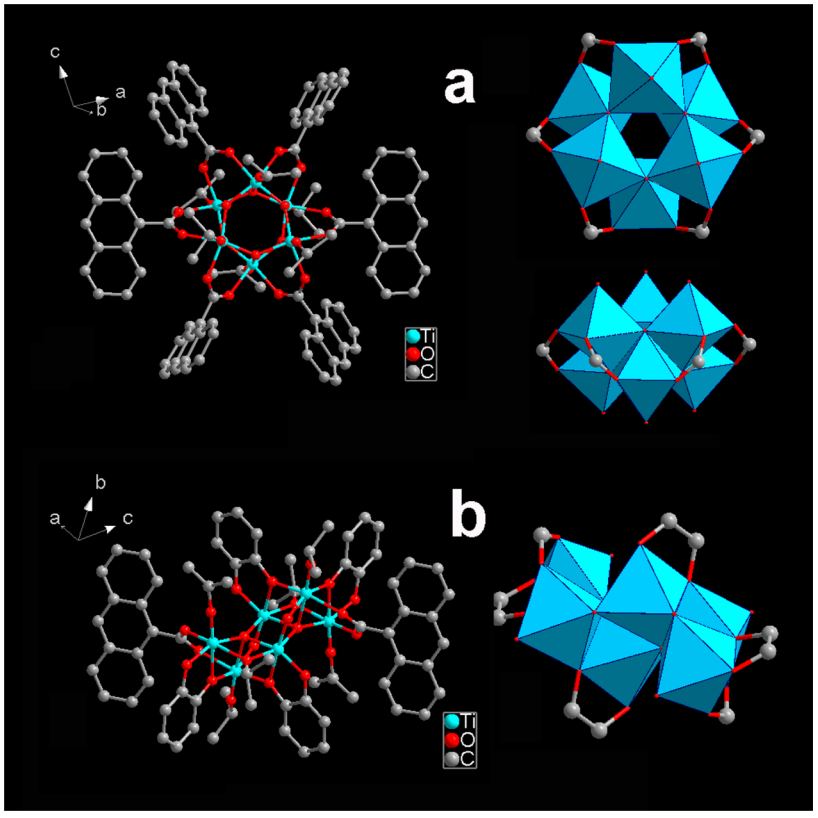

Figure 2. Molecular structures of (a) $[Ti_6O_6(O^iPr)_6(9\text{-AC})_6]$ (**1**) and (b) $[Ti_6O_4(O^iPr)_6(cat)_4(9\text{-AC})_2]$ (**2**), along with polyhedron views of the cluster structures. Hydrogen atoms are omitted for clarity.

dx.doi.org/10.1021/ic500390j | Inorg. Chem. 2014, 53, 7233−7240

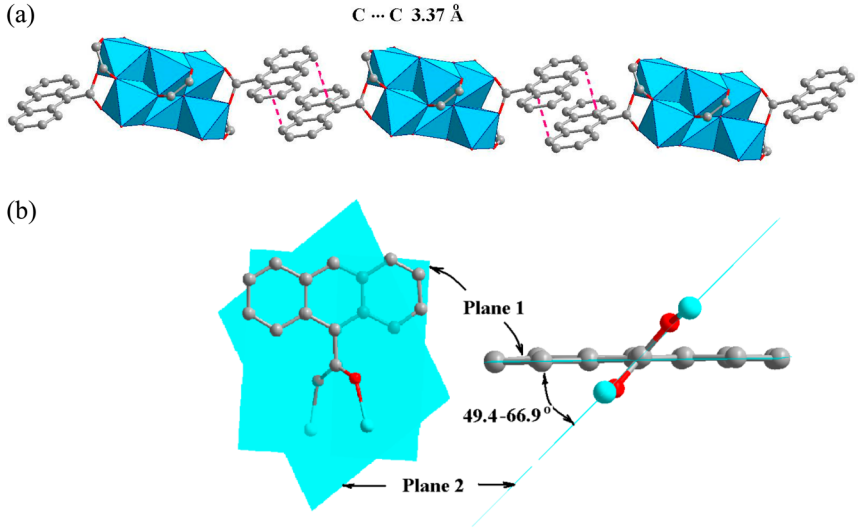

Figure 3. (a) One-dimensional structure assembled by $\pi\cdots\pi$ stacking of the anthracene planes in cluster **2**. (b) Views of dihedral angle between the AC plane and $C(OTi)_2$ plane.

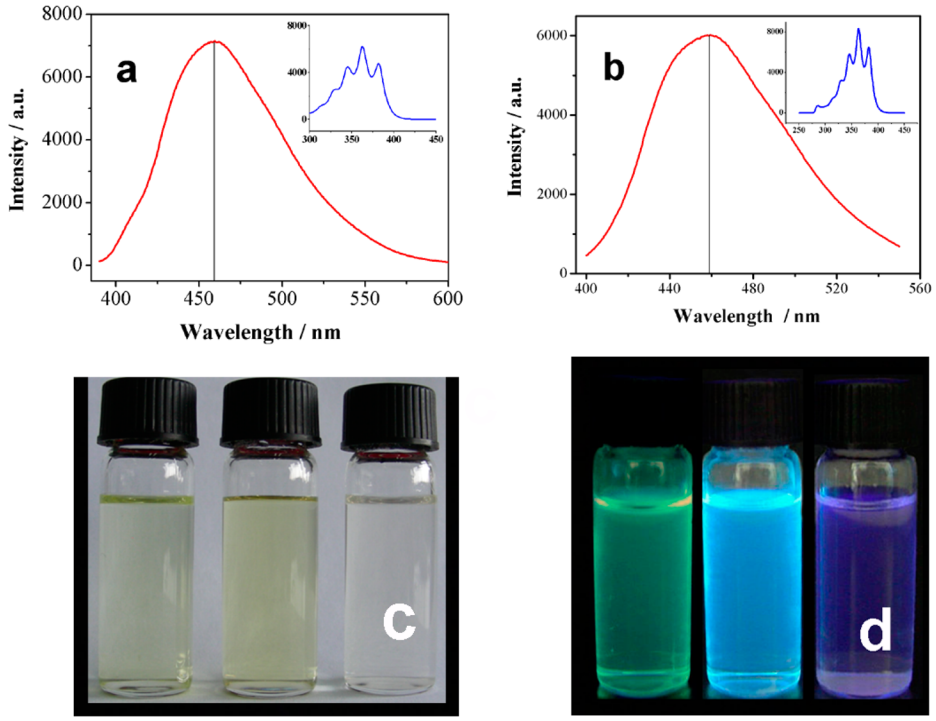

Figure 4. Fluorescence emission spectra of (a) **1** and (b) **2** measured with 360 nm excitation in dichloromethane, along with the excitation spectra (inset). (c, d) Photos of the solutions and their fluorescence images of cluster **1** in different solvents: dichloromethane (left), acetonitrile (middle), and diluted ammonia–water (right).

between the anthracenes. Similarly, one-dimensional structure is also found in **1**, but the $\pi\cdots\pi$ stacking distance is 3.597 Å. All the 9-AC ligands in **1** and **2** are coordinated to the TiO core in the same mode. The carboxyl group bonds to two apexes of two neighboring octahedra and the dihedral angle between the anthracene plane and $C(OTi)_2$ plane is in the range from 49.4(1)° to 66.9(1)°(Figure 3b). This angle is the balance of the best space filling (steric hindrance of H atoms) and the best electron conjugation for AC plan and the cluster.

Fluorescence Properties and Photodegradation. Fluorescence spectra of clusters **1** and **2** are shown in Figure 4a,b. The emission spectra of 9-AC and catechol can be found in Figure S5 (Supporting Information). The peak of **1** shifting from 465 nm of the 9-AC to 457 nm indicates the charge transfer from 9-AC to the cluster core in **1**. Photos of cluster **1** in different solvents, CH_2Cl_2, CH_3CN, and diluted ammonia–water, and their fluorescence emission are shown in Figure 4c,d. Solvent-induced sharp fluorescence change was observed, which should be assigned to the solvent intervention on the frontier orbital. The energy gaps are related to the dipole moment of the solvents in the order CH_2Cl_2 (3.4, dipole moment) < CH_3CN (6.2) < H_2O (10.2). The fluorescence quantum yields of clusters **1** and **2** are 0.077 and 0.061, significantly lower than that of the AC [$\Phi_F(s) = 0.27$],[15] which

dx.doi.org/10.1021/ic500390j | Inorg. Chem. 2014, 53, 7233–7240

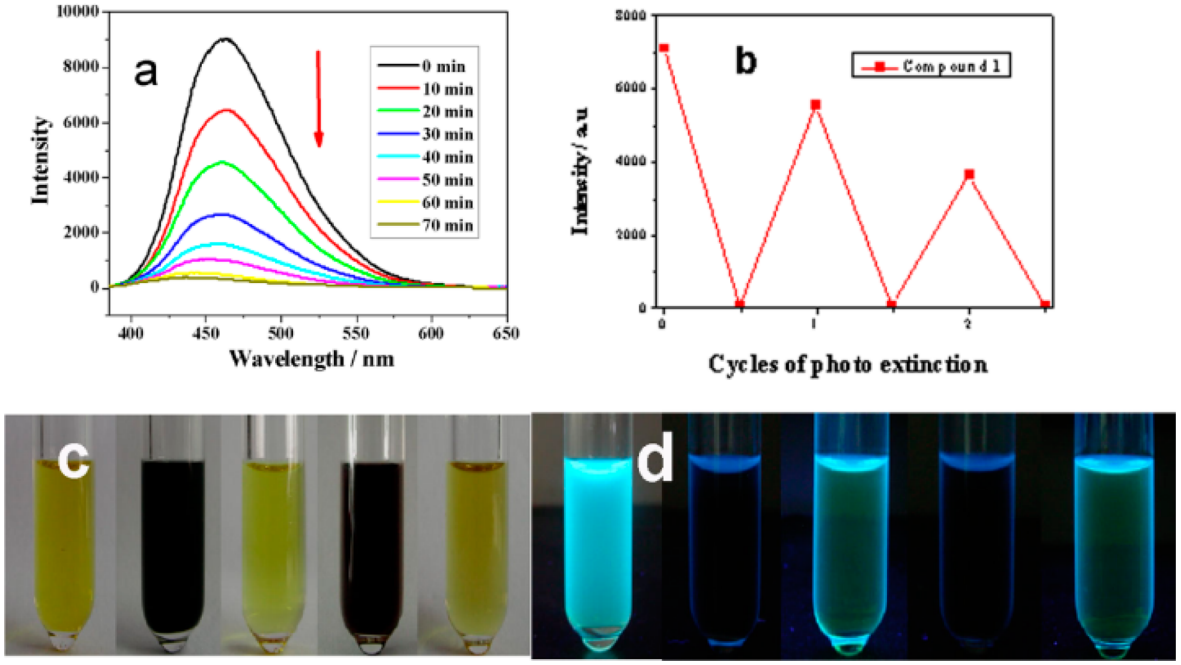

Figure 5. (a) Fluorescence intensity of **1** in dichloromethane (1.0×10^{-4} mol·L^{-1}) upon irradiation. (b) Fluorescence intensity of **1** upon alternate irradiation and oxygen bubbling. (c, d) Photos of the solutions and fluorescence images of **1** in dichloromethane upon alternate irradiation and oxygen bubbling (two cycles from left to right).

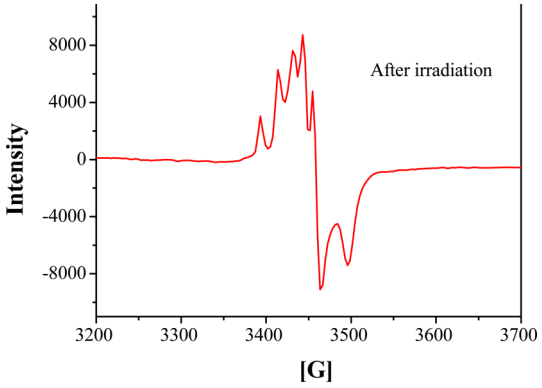

Figure 6. ESR spectrum of cluster **1** after irradiation (recorded at 110 K).

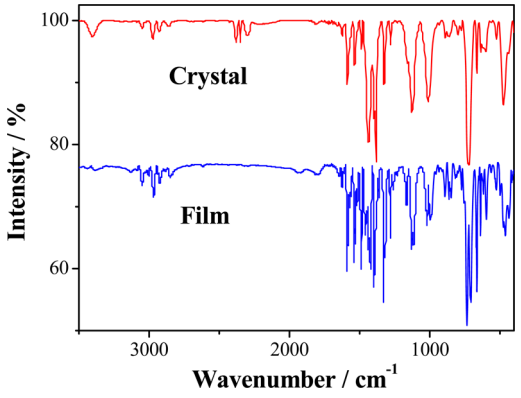

Figure 7. IR spectra of cluster **1** and the film of **1**.

proved the energy transition from excited AC group to TiO clusters. Figure S6 (Supporting Information) provides the fluorescence emission decays monitored at 420 nm after excitation at 360 nm in dichloromethane in the time window 900 μs.

Figure 5a shows the fluorescence spectra of **1** in dichloromethane (1.0×10^{-4} mol·L^{-1}) upon irradiation with a 70-W halogen lamp. The fluorescence becomes completely extinct in about 1 h. The fluorescence can be recovered very quickly by bubbling oxygen into the solution; however, the intensity gradually decreases with the number of on−off cycles (Figure 5b). Photos of the solutions and fluorescence images of **1** in dichloromethane upon alternate irradiation and oxygen bubbling are shown in Figure 5c,d. The dark color of the solution is the character of photoinduced Ti(III) that has been detected by electron spin resonance (ESR) for the fluorescence extinction system. The ESR spectrum (Figure 6) displays the signals of paramagnetic Ti(III) center in a distorted octahedral coordination field with parameters 1.939 (g_1), 1.961 (g_2), and 1.981 (g_3).[6c,d,16,17] The extinction phenomenon can be reasonably explained by the photoinduced reduction from Ti(IV) to Ti(III) that acts as a fluorescence quencher. It is well-known that TiO_2 has applications as a photocatalyst for the decomposition of organic dyes. Therefore, in the circulation part of the dye molecules is decomposed by the photoinduced Ti(III) centers. These results tell us that the TOC is also an effective photocatalyst, which can be used as a homogeneous catalyst (in solution) to eliminate the adsorbed aromatic ring compounds. Results of the degradation experiments for excessive 9-AC are given in Supporting Information (Figure S7). Nevertheless, the dye degradation problem should be considered in real dye-sensitized solar cells.

Photocurrent Responses. The photocurrent conversion property of the clusters was examined by use of a three-electrode cell with the cluster film-coated ITO electrodes. All the experiments were carried out in a 0.10 mol·L^{-1} Na_2SO_4 electrolyte solution under illumination with a 150-W high-pressure xenon lamp (a more detailed description is given in the Experimental Section). The films on electrode were

dx.doi.org/10.1021/ic500390j | Inorg. Chem. 2014, 53, 7233−7240

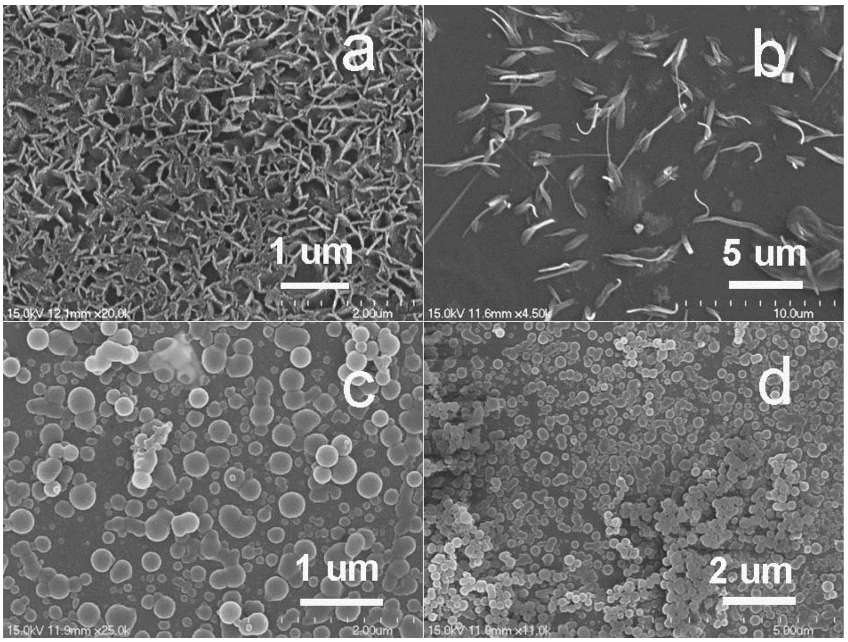

Figure 8. SEM images of the morphologies of the films of clusters (a, b) **1** and (c, d) **2**, prepared from dichloromethane solution in different concentrations.

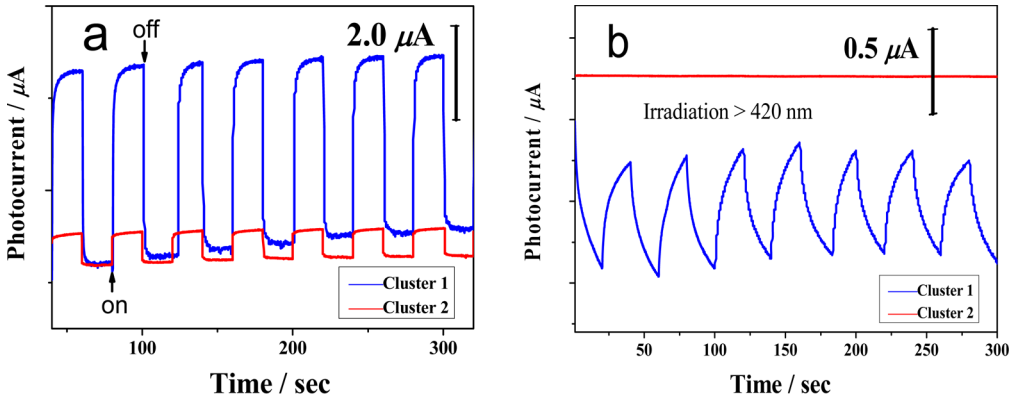

Figure 9. Photocurrent responses of **1** and **2** electrodes, (a) without and (b) with 420 nm filter.

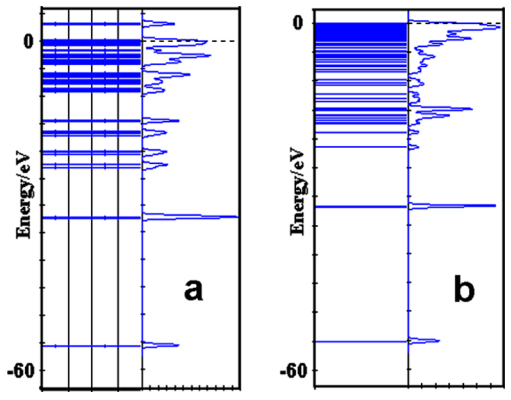

Figure 10. Band energy and total DOS of (a) unfunctionalized Ti_6O_{24} cluster and (b) cluster **1**.

characterized by IR spectra (Figure 7). The spectrum is compared with that of the crystal **1**. They are very similar to each other. Hydrolysis may usually happen in the preparation of the film due to the humidity in air, but it is not very serious in this case, which means the fundamental structure does not change significantly. Figure 8 shows the morphologies of clusters **1** (panels a and b) and **2** (panels c and d) on electrodes obtained by direct solution-coating method. Plate- or beltlike morphologies for cluster **1** and microspheres for cluster **2** were recorded. Upon repetitive irradiation, a clear photocurrent response was observed (Figure 9a). The anodic photocurrent was quickly reached and was stable without a decrease in intensity, demonstrating the photophysical stability and the good photoelectric response of the film during the experimental period. As shown in Figure 9a, the photocurrent of cluster **1** electrode is about 4.3 μA, a 6 times increase in comparison with that of cluster **2** electrode (0.72 μA), which benefits from the multiantenna effect of **1**. Comparatively good photocurrent behavior under visible irradiation would be expected for the red cluster **2** electrode due to its intense visible absorption. The short energy light was cut by a 420 nm filter and the result is shown in Figure 9b. Unexpectedly, no response of cluster **2** electrode was observed on the microampere scale. In contrast, weak response and zigzag current curve was obtained for cluster **1** electrode. The results indicate that catecholate is not a good photosensitizer. The excited electrons in Cat could not be

dx.doi.org/10.1021/ic500390j | Inorg. Chem. 2014, 53, 7233−7240

effectively injected into the cluster, which may be due to the energy mismatch problem. It is attributed to the extended absorption of the AC group, the on-set energy of cluster **1** being 456 nm. XPS spectra of the films before and after irradiation are measured, but the results only give the same signals (Figure S8, Supporting Information). No Ti(III) signal is detected that means the photoinduced electron−hole separation is an instant process.

Density of states (DOS) for cluster **1** (a simplified model based on crystal structure data, in which all the O^iPr groups were replaced by OH groups) were calculated by use of Materials Studio.[18] The total DOS is reproduced in Figure 10 together with that of the unfunctionalized Ti_6O_{24} cluster. There is clearly a band structure change between the Ti_6O_{24} cluster and the 9-AC-modified Ti_6O_{24} cluster. The discrete energy gap, from −9 to −14 eV, of the Ti_6O_{24} cluster gains a number of new energy levels due to the contribution of 9-AC molecules and the band structure turns to densification and overlapping, which is a feature often associated with efficient electron transfer in low-energy irradiation.

CONCLUSION

In summary, we prepared two TOC compounds, $[Ti_6O_6(O^iPr)_6(9\text{-AC})_6]$ (**1**) and $[Ti_6O_4(O^iPr)_6(cat)_4(9\text{-AC})_2]$ (**2**), with a photoactive ligand 9-anthracenecarboxylate by one-step in situ solvothermal synthesis. Cluster structures, TOC−anthracene group linkage, and molecular arrangements are characterized by single-crystal analysis. The fluorescence of the 9-AC-modified cluster is sensitive to the polarity of the solvents and can be turned off and on by irradiation and oxygen oxidation. The photoinduced Ti(III) is responsible for fluorescence extinction and dye degradation. The latter problem should be considered in the real dye-sensitized solar cells. The photocurrent conversion property of the clusters indicates that 9-AC is an effective photosensitizer and cluster **1** shows higher photocurrent intensity for its multiantenna dye structure. The energy band structure of the TOC is modified by coordination of 9-AC. It is very rare that TOCs are modified with fluorescence antennae and used as precursors in the preparation of photoactive electrodes.

ASSOCIATED CONTENT

Supporting Information

Eight figures showing FT-IR spectra, experimental and simulated XRD patterns, thermogravimetric measurements, molecular structures, fluorescence emission, degradation experiments for excessive 9-AC, and XPS spectra for **1** and **2** and one table listing crystal data and structural refinement parameters for **1** and **2** (PDF); crystallographic files for **1** and **2** (CIF). This material is available free of charge via the Internet at http://pubs.acs.org.

AUTHOR INFORMATION

Corresponding Authors

*E-mail: zhuqinyu@suda.edu.cn.
*E-mail: daijie@suda.edu.cn.

Notes

The authors declare no competing financial interest.

ACKNOWLEDGMENTS

We gratefully acknowledge financial support by the NSF of China (21371125), the Education Committee of Jiangsu Province (11KJA150001), the National College Student Innovation Project, and the Priority Academic Program Development of Jiangsu Higher Education Institutions.

REFERENCES

(1) (a) O'Regan, B.; Grätzel, M. *Nature* **1991**, *353*, 737−740. (b) Grätzel, M. *Nature* **2001**, *414*, 338−344. (c) Hagfeldt, A.; Grätzel, M. *Acc. Chem. Res.* **2000**, *33*, 269−277.

(2) (a) O'Regan, B. C.; Durrant, J. R. *Acc. Chem. Res.* **2009**, *42*, 1799−1808. (b) Labat, F.; Bahers, T. L.; Ciofini, I.; Adamo, C. *Acc. Chem. Res.* **2012**, *45*, 1268−1277 and references cited therein. (c) Mosconi, E.; Yum, J.-H.; Kessler, F.; García, C. J. G.; Zuccaccia, C.; Cinti, A.; Nazeeruddin, M. K.; Grätzel, M.; Angelis, F. D. *J. Am. Chem. Soc.* **2012**, *134*, 19438−19453. (d) Jeon, J.; Goddard, W.; Kim, H. *J. Am. Chem. Soc.* **2013**, *135*, 2431−2434. (e) Nayak, P. K.; Bisquert, J.; Cahen, D. *Adv. Mater.* **2011**, *23*, 2870−2876. (f) Mishra, A.; Fischer, M. K. R.; Bäuerle, P. *Angew. Chem., Int. Ed.* **2009**, *48*, 2474−2499.

(3) Grätzel, M. *Inorg. Chem.* **2005**, *44*, 6841−6851.

(4) (a) Duncan, W. R.; Prezhdo, O. V. *J. Am. Chem. Soc.* **2008**, *130*, 9756−9762. (b) Long, R.; English, N. J.; Prezhdo, O. V. *J. Am. Chem. Soc.* **2012**, *134*, 14238−14248. (c) Persson, P.; Bergström, R.; Ojamäe, L.; Lunell, S. *Adv. Quantum Chem.* **2002**, *41*, 203−263. (d) Persson, P.; Lunell, S. *Sol. Energy Mater. Sol. Cells* **2000**, *63*, 139−148. (e) Marotta, G.; Reddy, M. A.; Singh, S. P.; Islam, A.; Han, L.; Angelis, F. D.; Pastore, M.; Chandrasekharam, M. *ACS Appl. Mater. Interfaces* **2013**, *5*, 9635−9647.

(5) (a) Rozes, L.; Sanchez, C. *Chem. Soc. Rev.* **2011**, *40*, 1006−1030. (b) Rozes, L.; Steunou, N.; Fornasieri, G.; Sanchez, C. *Monatsh. Chem.* **2006**, *137*, 501−528.

(6) (a) Benedict, J. B.; Freindorf, R.; Trzop, E.; Cogswell, J.; Coppens, P. *J. Am. Chem. Soc.* **2010**, *132*, 13669−13671. (b) Sokolow, J. D.; Trzop, E.; Chen, Y.; Tang, J.; Allen, L. J.; Crabtree, R. H.; Benedict, J. B.; Coppens, P. *J. Am. Chem. Soc.* **2012**, *134*, 11695−11700. (c) Dan-Hardi, M.; Serre, C.; Frot, T.; Rozes, L.; Maurin, G.; Sanchez, C.; Ferey, G. *J. Am. Chem. Soc.* **2009**, *131*, 10857−10859. (d) Wu, Y.-Y.; Wen, L.; Wang, Y.-H.; Pu, Y.-Y.; Zhang, X.; You, L.-S.; Zhu, Q.-Y.; Dai, J. *Inorg. Chem.* **2012**, *51*, 8982−8988.

(7) (a) Benedict, J. B.; Coppens, P. *J. Am. Chem. Soc.* **2010**, *132*, 2938−2944. (b) Snoeberger, R. C.; Young, K. J.; Tang, J.; Allen, L. J.; Crabtree, H. H.; Brudvig, G. W.; Coppens, P.; Batista, V. S.; Benedict, J. B. *J. Am. Chem. Soc.* **2012**, *134*, 8911−8917. (c) Wu, Y.-Y.; Wang, P.; Wang, Y.-H.; Jiang, J.-B.; Bian, G.-Q.; Zhu, Q.-Y.; Dai, J. *J. Mater. Chem. A* **2013**, *1*, 9862−9868.

(8) (a) Zhang, J.; Lee, J.-K.; Wu, Y.; Murray, R. W. *Nano Lett.* **2003**, *3*, 403−407. (b) Zhu, L.; Al-Kaysi, R. O.; Dillon, R. J.; Tham, F. S.; Bardeen, C. J. *Cryst. Growth Des.* **2011**, *11*, 4975−4983. (c) Alberding, B. G.; Brown-Xu, S. E.; Chisholm, M. H.; Gustafson, T. L.; Reed, C. R.; Naseri, V. *Dalton Trans.* **2012**, *41*, 13097−13104. (d) Al-Kaysi, R. O.; Bardeen, C. J. *Adv. Mater.* **2007**, *19*, 1276−1280. (e) Khanra, P.; Kuila, T.; Bae, S. H.; Kim, N. H.; Lee, J. H. *J. Mater. Chem.* **2012**, *22*, 24403−24410.

(9) Srinivas, K.; Yesudas, K.; Bhanuprakash, K.; Rao, V. J.; Giribabu, L. *J. Phys. Chem. C* **2009**, *113*, 20117−20126.

(10) Teng, C.; Yang, X.; Yang, C.; Li, S.; Cheng, M.; Hagfeldt, A.; Sun, L. *J. Phys. Chem. C* **2010**, *114*, 9101−9110.

(11) (a) Rigaku Corporation, 1999. (b) *CrystalClear Software User's Guide*, Molecular Structure Corporation, 2000. (c) Pflugrath, J. W. *Acta Crystallogr. Sect. D* **1999**, *55*, 1718−1725.

(12) (a) Sheldrick, G. M. *SHELXS-97, Program for Structure Solution*, Universität of Göttingen, Germany, 1999. (b) Sheldrick, G. M. *SHELXL-97, Program for Structure Refinement*, Universität of Göttingen, Germany, 1997.

(13) (a) Tae, E. L.; Lee, S. H.; Lee, J. K.; Yoo, S. S.; Kang, E. J.; Yoon, K. B. *J. Phys. Chem. B* **2005**, *109*, 22513−22522. (b) Jeong, N. C.; Lee, J. S.; Tae, E. L.; Lee, Y. J.; Yoon, K. B. *Angew. Chem., Int. Ed.* **2008**, *47*, 10128−10132.

(14) (a) Boyle, T. J.; Tyner, R. P.; Alam, T. M.; Scott, B. L.; Ziller, J. W.; Potter, B. G. *J. Am. Chem. Soc.* **1999**, *121*, 12104−12112. (b) Piszczek, P.; Richert, M.; Wojtczak, A. *Polyhedron* **2008**, *27*, 602−608. (c) Pandey, A.; Gupta, V. D.; Nöth, H. *Eur. J. Inorg. Chem.* **2000**, 1351−1357. (d) Ammala, P. S.; Batten, S. R.; Kepert, C. M.; Spiccia, L.; Bergen, A. M.; West, B. O. *Inorg. Chim. Acta* **2003**, *353*, 75−81.
(15) (a) Alonso, R.; Yamaji, M.; Jiménez, M. C.; Miranda, M. A. *J. Phys. Chem. B* **2010**, *114*, 11363−11369. (b) Lakowicz, J. R. *Principles of Fluorescence Spectroscopy*; Springer Science Business Media: New York, 2006.
(16) Kuznetsov, A. I.; Kameneva, O.; Rozes, L.; Sanchez, C.; Bityurin, N.; Kanaev, A. *Chem. Phys. Lett.* **2006**, *429*, 523−527.
(17) (a) Prakash, A. M.; Kurshev, V.; Kevan, L. *J. Phys. Chem. B* **1997**, *101*, 9794−9799. (b) Murata, C.; Yoshida, H.; Kumagai, J.; Hattori, T. *J. Phys. Chem. B* **2003**, *107*, 4364−4373.
(18) *Materials Studio 4.0*, Accelrys Inc., Son Diego, CA, 2006.